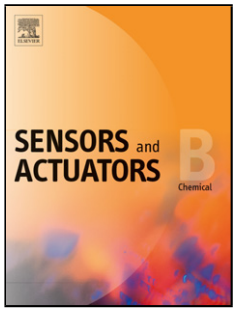


Title: Cell detection by surface imprinted polymers SIPs: A study to unravel the recognition mechanisms

Authors: Derick Yongabi, Mehran Khorshid, Patricia Losada-Pérez, Kasper Eersels, Olivier Deschaume, Jan D'Haen, Carmen Bartic, Jef Hooyberghs, Ronald Thoelen, Michael W*ü*bbenhorst, Patrick Wagner

PII: S0925-4005(17)31546-0
DOI: http://dx.doi.org/10.1016/j.snb.2017.08.122
Reference: SNB 22989

To appear in: *Sensors and Actuators B*

Received date: 26-4-2017
Revised date: 14-7-2017
Accepted date: 15-8-2017

Please cite this article as: Derick Yongabi, Mehran Khorshid, Patricia Losada-Pérez, Kasper Eersels, Olivier Deschaume, Jan D'Haen, Carmen Bartic, Jef Hooyberghs, Ronald Thoelen, Michael W*ü*bbenhorst, Patrick Wagner, Cell detection by surface imprinted polymers SIPs: A study to unravel the recognition mechanisms, Sensors and Actuators B: Chemicalhttp://dx.doi.org/10.1016/j.snb.2017.08.122

# Cell detection by surface imprinted polymers SIPs: A study to unravel the recognition mechanisms

Derick Yongabi [a, *], Mehran Khorshid [a, b], Patricia Losada-Pérez [b, c], Kasper Eersels [a], Olivier Deschaume [a], Jan D'Haen [b, c], Carmen Bartic [a], Jef Hooyberghs [d, e], Ronald Thoelen [b, c], Michael Wübbenhorst [a], Patrick Wagner [a]

[a] Soft-Matter Physics and Biophysics Section, Department of Physics and Astronomy, KULeuven, Celestijnenlaan 200D, B-3001, Leuven, Belgium

[b] Institute for Materials Research IMO, Hasselt University, Wetenschapspark 1, B-3590, Diepenbeek, Belgium

[c] IMEC vzw, division IMOMEC, Wetenschapspark 1, B-3590, Diepenbeek, Belgium

[d] Flemish Institute for Technological Research, VITO, Boeretang 200, B-2400 Mol, Belgium

[e] Theoretical Physics, Hasselt University, Agoralaan - Building D, B-3590, Diepenbeek, Belgium

[*]Corresponding author:

Derick Yongabi

Phone: +32 – 16 – 32 78 42. E-mail: derick.yongabi@kuleuven.be

**Graphical Abstract**

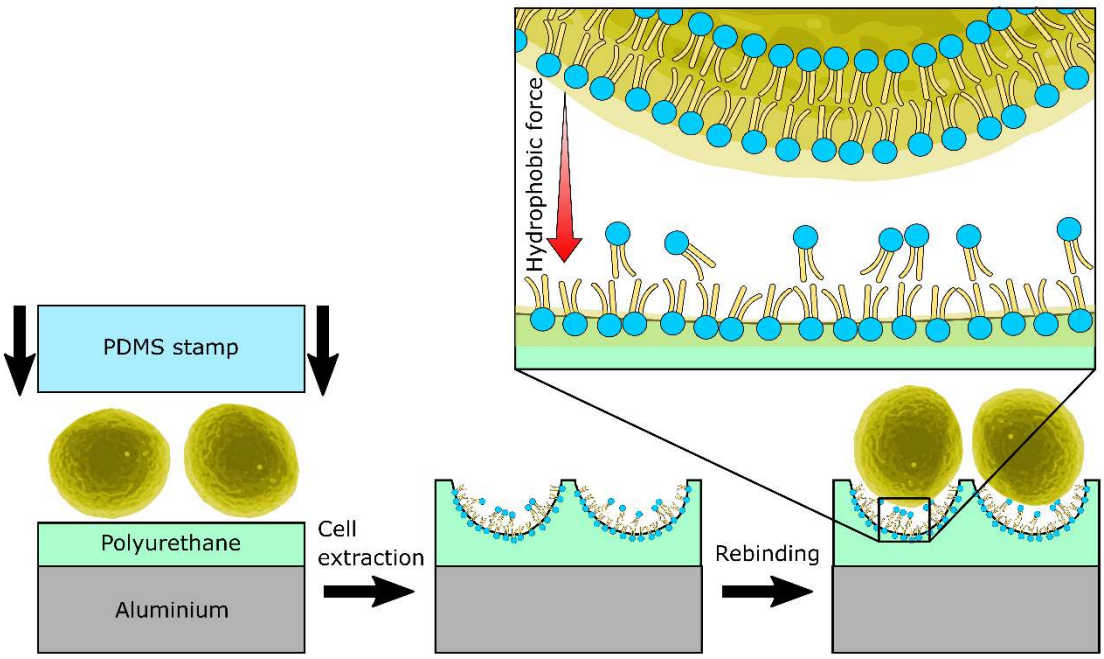


Highlights

- The mechanisms responsible for the selective recognition of cells by surface-imprinted polymers (SIPs) have been examined.
- We have shown that the recognition of cells by SIPs depend partly on the geometrical matching between template cells and imprinted cavities on the SIP layer as well as interactions with phospholipid moieties incorporated into the SIP cavities.
- The phospholipids play a significant role in the cell-SIP binding mechanism through long range hydrophobic forces while SIP-imbedded proteins do not seem to play a role.

## Abstract

Previous studies have shown that selective synthetic cell receptors can be produced by cell imprinting on polymer layers. However, knowledge on the fundamental detection mechanisms remains limited. In this article, while using yeast cells (*Saccharomyces cerevisiae*) as model cells, the factors influencing cellular recognition by surface-imprinted polymers (SIPs) are studied by means of spectroscopic and microscopy techniques and a transducer platform based on interfacial thermal transport, the so-called heat-transfer method (HTM). These analyses indicate that cell imprinting creates selective binding sites on the surface of the SIP layer in the

form of binding cavities that match the cells in shape and size. Also, we show that phospholipid moieties are incorporated into the SIP cavities during imprinting, while membrane proteins do not seem to be transferred. More importantly, we demonstrate that the incorporated phospholipids significantly enhance cell adhesion to the SIP, and thus play a significant role in the cell-SIP binding mechanism. Furthermore, the hydrophobicity of the SIP layer was found to be considerably higher when compared with a non-imprinted polymer layer (NIP), an effect that could not be attributed to the presence of cavities on the surface of the SIP layer. Therefore, we suggest that the role of phospholipids in the SIP recognition mechanism is mediated by long range hydrophobic forces.

Keywords: Cell detection; surface-imprinted polymers; cell adhesion; phospholipids; membrane proteins; biomimetic sensors.

## 1. Introduction

In many cases, the correct diagnosis of a disease depends on the specific identification of cells or pathogens contained in body fluids. Similarly, the prevention of large-scale outbreaks of infectious diseases does not only depend on personal hygiene, but also on the detection of pathogens such as bacteria and viruses in water, food and air. The most important cell detection techniques are based on polymerase chain reaction (PCR), oligonucleotide DNA microarrays, microscopy, flow cytometry, fluorescent *in situ* hybridization, and pyrosequencing [1-6]. Although these techniques are very sensitive, they require expensive equipment that have to be used in a lab environment by trained personnel. It is therefore desirable to develop portable, low-cost systems that are able to detect cells or pathogens in a fast and selective manner.

An interesting approach to construct such devices is to incorporate surface imprinted polymers (SIPs), acting as biomimetic cell receptors into sensor platforms [7]. SIPs can be made via several approaches and have been imprinted with various templates including proteins [8-

10], yeast [11, 12], viruses [13, 14], bacteria [15, 16], and mammalian cells [17, 18]. SIP-covered electrodes are typically combined with low-cost, user-friendly readout platforms based on microgravimetric [19-21], electrochemical [22-24], optical [25, 26], and thermal transducer principles [27-29]. One of the most interesting surface imprinting approaches is the so-called stamping or microcontact printing approach, where a layer of template cells is applied onto the surface of a stamp. The stamp is then pressed onto a semi-cured polymer layer which is prepared in parallel on a suitable substrate material. During curing, the polymer is crosslinked around the cells. After removal of the cells, microcavities are left behind on the surface of the polymer that are able to rebind the template [11, 18].

In addition to their low-cost, straightforward synthesis procedure, superior thermal, physical and chemical stability as well as their regenerative capacity [30], SIPs display remarkable selectivity for their targets. However, the rebinding mechanisms driving this selectivity are not fully understood yet. It has been suggested that curing the polymer in the presence of template cells initiates the organization of the polymer chains around the templates, such that the geometrical and chemical information of the cell surface is captured by the polymer, which in turn creates binding sites on the polymer surface with high affinity and selectivity for the template cells [31, 32]. However, these claims are rather suggestive, therefore, an in-depth study is required to unveil the working mechanisms that enable these receptors to selectively rebind their targets.

In this article, the factors influencing the recognition of cells by their corresponding SIPs will be explored using yeast cells (*Saccharomyces cerevisiae*) as model cells as they are robust, readily available and were the first to be used for microcontact printing [11,12]. Our preliminary hypothesis is that geometric compatibility and complementary functional groups on lipids and proteins, transferred from the cell membrane to the SIP layer play a major role in the recognition

mechanisms. To investigate this, morphological analysis of the receptor layers by atomic force microscopy (AFM) and scanning electron microscopy (SEM) was carried out before and after cell detection events to study the transfer of geometrical information to the imprints. The wetting behavior of the SIP receptor was evaluated using water contact angle analysis, while Fourier transform infrared spectroscopy (FTIR) and X-ray photoelectron spectroscopy (XPS) were used to identify whether cell membrane entities are transferred to the SIP layer during imprinting. In order to gain insight into the role of transferred membrane remnants (particularly proteins and phospholipids) on cell-SIP binding, SIP layers were created using different strategies and cell-rebinding was studied in real time using the heat-transfer method. To study the role of proteins, SIP layers were exposed to pepsin to degrade any SIP-embedded proteins and the effect of this treatment on the performance of the SIP layer was evaluated. Additionally, a polyurethane layer was imprinted with phospholipid vesicles (dipalmitoylphosphatidylcholine, DPPC) to determine if phospholipids drive SIP-based cell detection.

## 2. Materials and Methods

### 2.1 Surface imprinting

Polydimethylsiloxane (PDMS) stamps were used to imprint template material (cells, lipid vesicles and silica beads) on polyurethane layers. The PDMS stamps were synthesized using the Sylgard 184® elastomer kit (Malvom N.V., Schelle, Belgium). Yeast cells (*S. cerevisiae*) used for imprinting were prepared by suspending baker's yeast from Dr. Oetker (Bielefeld, Germany) in phosphate buffered saline (PBS). A cell concentration of 10 mg/ml was used for imprinting. In addition, a 5 mg/ml-suspension of 2.0 μm-mesoporous silica beads in water (molecular weight = 60.08 g/mol, 99.9% purity, pore size ≈ 2 nm, Sigma-Aldrich, Diegem, Belgium) was used for creating silica bead imprints.

Lipid vesicles were prepared by dissolving DPPC (Avanti Polar Lipids, Alabaster, USA) in chloroform stabilized with 0.6% ethanol. A lipid film was produced by evaporating chloroform under a gentle nitrogen flow and later storing it for 15 hours in a nitrogen atmosphere to remove any remaining solvents. The dry lipid film was then hydrated with 4-(2-hydroxyethyl)-1-piperazineethanesulfonic acid buffer [HEPES (10 mM HEPES (99%) and 150 mM NaCl (≥ 99.5%) Sigma-Aldrich, Diegem, Belgium), pH 7.4] to 1 mg/ml with continuous stirring to form large multilamellar vesicles (LMVs). SEM images of the vesicles indicate that they aggregated in time to form ≈ 400 nm-size vesicles prior to imprinting. To control the temperature of the lipids during hydration, the lipid-containing flask was suspended in a water bath at a temperature of 56 °C, which is considerably higher than the DPPC melting temperature, $T_m \approx 41$ °C [33].

The SIPs for cell detection were created by depositing a layer of yeast onto a PDMS stamp. A 10 mg/ml cell suspension was applied on the stamp and the cells were left to sediment for 30 mins. Afterwards, the cells were spin-coated on the stamp at 3000 rpm for 60 seconds with an acceleration of 1000 rpm/s to produce a uniform and dry monolayer of cells. Sedimentation and spin coating were performed at room temperature. All subsequent steps were performed under an inert nitrogen atmosphere. The polyurethane synthesis protocol has been described by the authors in previous work [18]. The prepolymerization mixture was made by dissolving 122 mg of the initiator 4,4'- diisocyanatodiphenylmethane, 222 mg of the polyol monomer bisphenol A, and 25 mg of the phloroglucinol, serving as crosslinker, in 500 µl of anhydrous tetrahydrofuran (THF). All these reagents were used as received from Sigma Aldrich N.V. (Diegem, Belgium) and had a purity of at least 99.9 %. Nucleophilic addition polymerization was initiated thermally at 65 °C. The mixture was cured until the gelling point was reached (± 180 minutes) and diluted 5x in THF for spin coating. A thin layer (thickness ≈ 1.2 µm) of the polymer gel was deposited onto an aluminum chip (1 cm × 1 cm, Brico N.V.,

Korbeek-Lo, Belgium) by spin coating for 60 seconds at 2000 rpm, and 1000 rpm/s. Afterwards, the template-covered PDMS stamp was pressed onto the polyurethane layer with a pressure of about 70 Pa and the ensemble kept for 18 hours at 65 °C for the polymer to fully cure and interact with the template cells. Finally, the stamp was removed and the bound template cells were washed off the chip using a 1 % sodium dodecyl sulfate (SDS) solution. Imprints for lipid vesicles and silica beads were prepared using the same protocol. Non-imprinted polymer layers (NIPs), used for reference measurements, were prepared identically but using a non-loaded stamp. More details can be found in reference 18.

To evaluate the potential role of proteins on the SIP-based cell recognition mechanism, both a SIP and a NIP were treated with a pepsin solution to remove all proteins from the surfaces. The pepsin enzyme solution (pH 2) was prepared as recommended by the supplier; 0.4 % pepsin (Sigma Aldrich) in 10 mM hydrochloric acid (PROLABO®, Paris, France). After washing the chips in 1 % SDS and rinsing them with a phosphate buffered saline solution (1 x PBS), they were gently dried with nitrogen gas before being covered with the pepsin solution. Next, they were left for one hour at 37 °C to activate the pepsin enzyme. Finally, the chips were washed and rinsed again with PBS to prepare them for use.

### 2.2 Morphological analysis

The transfer of geometrical information to the imprints was analyzed using SEM and AFM. AFM measurements were performed in non-contact mode using a NX 10 AFM (Park Instruments, Suwon, South Korea) equipped with standard pyramidal-shaped silicon nitride ($Si_3N_4$) cantilever tips (length, 125 µm) with a nominal spring constant of 40 N/m (ST Instruments, Sliedrecht, The Netherlands). SEM imaging was performed using a FEI Quanta 200F-scanning electron microscope (FEI, Hillsboro, Oregon, USA). The surfaces of all substrates were carbon-coated to create thin conductive layers prior to the measurements.

### 2.3 Contact angle measurements

The wetting properties of the SIP (imprinted with cells and silica beads) and NIP layers were evaluated by contact angle measurements using an optical contact angle device (Data Physics OCA, Lancashire, UK). Measurements were performed at room temperature using a 5 µm-diameter water drop at a dosing rate of 1.00 µl/s. For each substrate, the contact angle was determined by taking the mean of four measurements performed at four positions on the chip. Prior to the measurements, all the chips, except the non-extracted yeast SIP were washed in SDS and rinsed with Milli-Q.

### 2.4 Chemical analysis

To analyze the chemical functionalities within the cavities of the SIP, XPS was used alongside FTIR. For XPS, an Al $K_\alpha$ X-ray source was used to determine the surface chemical composition by scanning the surface for binding energies ranging from 80 eV to 200 eV (SPECS® PHOIBOS 100MCD-5, Berlin, Germany). This is the region where phosphorus 2s and $2p_{3/2}$ peaks are located. On the other hand, FTIR spectra were acquired in specular reflectance at 60° using a Nicolet™ iS™ 5 FTIR Spectrometer (Thermo Scientific™ Inc., Massachusetts, USA). A blank aluminum substrate was used for background measurements. For each sample, 128 scans at a resolution of 4 $cm^{-1}$ were used to collect absorption spectra. The OMNIC™ Spectra Software (Thermo Scientific™ Inc.) was used to collect and analyze the spectra.

### 2.5 HTM measurements

The interaction of cells with SIPs and NIPs was monitored using the HTM setup [18]. The sensor chip was mounted in a custom made 110 µl-microfluidic flow cell using an O-ring as a water tight seal. The O-ring defines a contact area of 28 $mm^2$ between the sensor surface and the liquid in the flow cell. The backside of the substrate, consisting of polished aluminum, was mechanically fixed to a copper block, which serves as a heat source, heated by a 22 Ω

power resistor (MPH20, Farnell, Belgium). During measurements, the sensor surface was exposed to cells using an automated pump-driven syringe (ProSense, NE-500, The Netherlands). Two 500 µm K-type thermocouples (TC Direct, The Netherlands), were used to monitor the temperature of the copper block ($T_1$) and the temperature of the liquid at the center of the flow cell ($T_2$). A software-based proportional-integral-derivative controller (PID) was used to maintain the temperature of the copper block at a constant temperature of 37 °C during the entire experiment. All measurements were performed at a room temperature of 19.0 °C. **Figure 1** shows a schematic diagram of the HTM setup.

During all measurements, the temperature of the copper block was first stabilized in PBS buffer for 20 minutes before injecting a yeast cell suspension (10 mg/ml) into the flow cell at a rate of 2.5 ml/min for 72 seconds. The system was left to stabilize again for 20 minutes before being flushed with PBS at a rate of 0.25 ml/min for 12 minutes to remove all non-specifically bound cells. This was followed by a final 20-minute stabilization step. Cell recognition is based on the premise that bound cells on the substrate layer impede thermal transport, resulting in a decrease in the liquid temperature $T_2$. By monitoring $T_2$, the time evolution of the heat transfer resistance, $R_{th}$, is determined from the temperature difference ($T_1$-$T_2$) and the power P, required to maintain the copper block at the requested temperature (equation 1).

$$R_{th} = \frac{(T_1 - T_2)}{P} \qquad (1)$$

The origin of the thermal resistance of cells is not completely clear. However, lipid bilayers have been reported to exhibit a high thermal resistance that is significantly higher than that of bulk water [34]. Therefore, the high thermal resistance of cells can be partly attributed to their phospholipid bilayers. It is important to note that the heat-transfer resistance, $R_{th}$, is a device-specific quantity because a certain fraction of the heating power, P, dissipates to the ambient without passing through the sensitive surface.

## 3. Results and Discussion

### 3.1. HTM measurements on NIP and SIP

In a first series of experiments, the SIP's potential for reliably detecting yeast cells was assessed using a yeast SIP and a NIP. The SIP and NIP layers were exposed to yeast cells in the HTM setup and their responses were analyzed at $T_1$ = 37 °C ± 0.1 °C. **Figure 2** shows a comparison between the time-dependent thermal resistance of the NIP and the SIP in response to a 10 mg/ml suspension of target cells (yeast). The lower baseline level for the SIP layer can be attributed to the reduced thickness of the polymer within the imprinted cavities. In fact, the morphology of the imprints, discussed later in section 3.2, shows that some cavities are so deep that they almost touch the surface of the aluminum chip. As polyurethane is a thermal insulator, these cavities constitute preferential heat channels [18]. In both cases, the $R_{th}$ increases after injection of the cells, indicating cell attachment to the surface. However, the $R_{th}$ increase of 0.7 °C/W measured with a NIP is considerably lower than the $R_{th}$ increase of 2.0 °C/W measured with a SIP, thus indicating that the SIP has a higher binding affinity for the target cells. Following the rinsing step with PBS, the $R_{th}$ increase for the NIP layer decreases fully to the background level, while that for the SIP decreased to ≈ 20 %. This suggests that specific cell-binding occurs for the SIP, but not for the NIP.

### 3.2 Morphological analysis of imprints

A first step in understanding how cells bind to their imprints was performed by analyzing the morphology of the cavities in relation to the cells using AFM and SEM. **Figures 3a** and **3b** show AFM and SEM images of a yeast cell SIP prior to template extraction (non-extracted SIP). As shown, the surface is completely covered with yeast cells with an average diameter of 2.5 µm, which confirms that yeast cells are imprinted onto the polymer layer. **Figures 3c** and **3d** show the same polymer layer after extraction of the cells. The surface is fully covered with

imprinted spherical cavities with a surface coverage of approximately 8,250,000 cells per $cm^2$. In addition, the cavities are comparable to the cells in size and shape. Such shape and size matching of imprinted cavities with template cells has been reported in previous studies [18].

To gain further insight into the morphology of the cavities, a SEM image of a single cavity was acquired as displayed in **Figure 4**. The cavity is roughly spherical with its internal wall displaying nano-scale roughness. The origin and composition of these nano-scale features are not exactly clear, but left-over cell membrane fragments or a transfer of the cell's surface roughness to the polymer layer are plausible explanations.

Similar to the SIP made with yeast cells, a silica SIP was created using silica beads, which are inert and comparable in size to yeast cells (2 µm). The purpose of these imprints was to evaluate the relative contribution of the imprinted spherical cavities to the hydrophobicity of the SIP receptor layer. **Figure 5** shows the AFM image of the polyurethane layer produced after extraction of the silica beads. As shown, imprinting with silica beads yields cavities on the polymer layer that match in size and shape with the silica beads.

The geometrical matching of the cells and their imprints indicates that template cells are capable of binding into the imprinted cavities. To verify whether cells bind indeed into these cavities, a yeast SIP and NIP, which had been exposed to yeast cells in the HTM device and rinsed stringently with PBS were analysed by AFM and SEM. The images, shown in **Figure 6a** (AFM) and **6b** (SEM) reveal cells bound in the imprinted cavities of the SIP. Thus, imprinted cavities provide selective binding sites where cells bind strongly. On the contrary, **Figure 6c** shows the NIP layer void of cells, suggesting that the binding between cells and the NIP is weak, hence confirming that the imprinted cavities play a role in the selective recognition of the template cells by their corresponding SIP.

### 3.3 Effect of surface hydrophobicity

The results described in **Figure 6** suggest that the SIP cavities exhibit special properties that are responsible for their higher affinity towards the cells. One possible property is the hydrophobicity of the SIP surface. Indeed, it is well known that surface hydrophobicity enhances cell adhesion to surfaces through long range hydrophobic forces, with the extent and magnitude of these forces predictable from contact angle measurements [35,36]. For instance, the adhesion of *Candida albicans* (a species of yeast) on plastic surfaces and bacteria on polystyrene surfaces have been shown to increase with increasing water contact angle [37,38]. To confirm whether hydrophobicity plays a role in the ability of SIPs to strongly bind cells, contact angle measurements were performed on a non-extracted yeast SIP, yeast SIP, NIP and silica SIP. The average contact angles were respectively 37° ± 2, 92° ± 3, 75° ± 2 and 72° ± 2 (**Figure 7**). These values were determined from four measurements performed on different spots of the same sample. The contact angle of the non-extracted SIP can be assumed to be the contact angle of the template cells and is similar to the ones measured for other species of yeast such as *C. albicans* [39]. The low contact angle measured on this surface can be explained by the presence of large amounts of oxygen- and hydroxyl-rich moieties within the cell walls of *S. cerevisiae*, such as glucans (≈78%), chitins (≈37.3%) and mannoproteins (≈24.4), which make the cell surface hydrophilic [40]. The influence of the underlaying polyurethane layer on the contact angle can be assumed to be negligible because of the high surface coverage of the polymer-trapped template cells. Conversely, the higher contact angle measured on the NIP (75° ± 2) is comparable to the contact angle of 75° ± 1 measured on similar polyurethanes (polyethers) as expected [41]. The higher hydrophobicity of the NIP compared to the non-extracted SIP can be attributed to the fewer and more interspersed oxygen moieties of the polyurethane chains which are masked by the longer and predominant hydrophobic domains. Interestingly, the contact angle of the silica SIP (72° ± 2) is comparable to that of the NIP, thus,

suggesting that the measured value is more related to the polyurethane layer than to the spherical cavities embossed on the polymer layer. Therefore, it can be concluded that the morphological presence of the cavities does not significantly change the hydrophobicity of the surface. Most importantly, the contact angle measured on the yeast SIP is significantly higher as compared with the NIP and silica SIP. Thus, the strong binding between these hydrophobic layers and the template yeast cells described in **Figure 6** suggests that the wetting properties of the SIP layer play a major role in the mechanisms by which cells bind to SIP. However, the higher contact angle of this layer cannot be explained by the presence of the cavities themselves, as mentioned earlier, which implies that the hydrophobicity of the layer is due to chemical modifications by the cell-imprinting process itself. A possible hypothesis is that hydrophobic moieties from the cell-membrane, such as phospholipids, are incorporated into the cavity surface, increasing its hydrophobicity and thereby increasing the contact angle.

### 3.4 Identification of chemical groups transferred to the SIP layer

In order to identify the chemical moieties that are potentially transferred to the imprinted cavities, all surfaces were analyzed using FTIR and XPS to check for the presence of the main components of a cell membrane; phospholipids and membrane proteins. **Figure 8** shows the FTIR spectra of a NIP (red), a yeast SIP (purple), and a non-extracted yeast SIP (blue). The latter shows very high absorbance peaks at wavenumbers characteristic of proteins and lipids as expected, due to the presence of cells on its surface. More specifically, the O-H stretching vibrations at 3550 $cm^{-1}$ (proteins, phosphates and bonded water), C-H stretching of $sp^3$ carbons (2873 $cm^{-1}$, 2933 $cm^{-1}$ and 2966 $cm^{-1}$), C-H stretching of $sp^2$ carbons (3064 $cm^{-1}$ and 3034 $cm^{-1}$) and secondary amides (amide I at 1596 $cm^{-1}$ and amide II at 1613 $cm^{-1}$). However, the secondary amide bands, which are part of a typical protein signature, are also present in polyurethane spectra [42]. Therefore, their presence on the SIP would give little information regarding the transfer of proteins.

In addition, the occurrence of C=O stretching vibration bands around 1725 $cm^{-1}$ indicates the presence of carboxylic acids, amides or esters. As depicted in the inset of **Figure 8**, a double carbonyl peak occurs in the spectrum acquired from the non-extracted SIP. On the other hand, the NIP and SIP spectra show single and smooth peaks. The extra carbonyl peak can be attributed to the C=O stretching in carboxylic acids in proteins, suggesting that there may be no proteins on the SIP and NIP. Most importantly, carboxylic acids produce a characteristically broad absorption band in the 2500 – 3300 $cm^{-1}$ range (O-H stretching), which overlaps with the C-H bands. This band is clearly visible on the non-extracted SIP's spectrum, unlike the SIP and NIP whose OH bands are rather narrow, smooth and clearly distinct from the C-H bands. Therefore, based on these observations, it is unlikely that proteins are left on the SIP layer.

To examine the presence of lipids on the SIP layer, the NIP spectrum was subtracted from the SIP spectrum. **Figure 9a** shows the result of this subtraction. The peak extending above and below 2600 $cm^{-1}$ can be attributed to an O-H stretching absorption band. Bands in this region (2780 to 2630 $cm^{-1}$) have been well characterized as the P-OH stretches in highly hydrogen-bonded acid forms of phospholipids [43]. This indicates that molecules of a lipid-nature might be present on the SIP. Furthermore, the occurrence of this peak at lower wave numbers reveals more information about the nature of the phospholipids and the type of bonding between the lipids and the polymer. For instance, acidic lipids form strong hydrogen bonds and have FTIR peaks in the region between 2780 to 2630 $cm^{-1}$ [44]. Such lipids normally contain covalently bonded OH groups, giving them the ability to form strong hydrogen bonds. The cell membrane of *S. cerevisiae* contains several of these acidic lipids, *e.g.* phosphatidylethanolamine, phosphatidic acid and cardiolipin [45]. Ionized lipids on the other hand contain OH groups from bound water and their OH absorption bands are in the spectral region between 3430 and 3330 $cm^{-1}$ [46]. These results clearly suggest that lipids are transferred from the cell membrane to the SIP during the imprinting process. To gain more insight into the presence and nature of

phospholipids on the SIP layer, an analysis of the phosphate region of the spectrum (800 and 1300 $cm^{-1}$) was performed. In this region, $PO_2^-$, P=O, and P–O–C absorption bands are unique for all phospholipids [47]. As shown in **Figure 9b**, peaks occur at 1080 and 1232 $cm^{-1}$, which can be assigned to the symmetric and asymmetric phosphate diester stretches respectively in the central $PO_2^-$ group [48, 49]. In addition, the absorption peak at 1180 $cm^{-1}$ can be associated with the symmetric ester C–O–P stretch in C–O–$PO_2^-$, while the peaks at 1035 $cm^{-1}$ and 1014 $cm^{-1}$ belong to the symmetric ester P–O–C and P-OH stretches, respectively [47, 50]. The existence of the characteristic phospholipid peaks (P=O, $PO_2^-$ and P–O–C) in this region strongly suggests that phospholipids are transferred to the SIP layer.

With regard to the nature of the lipids, the peaks in the region between 1180 $cm^{-1}$ and 1080 $cm^{-1}$ have been reported to belong to acidic phosphates, thus supporting the assignment of the peak at 2600 $cm^{-1}$ to OH stretching in acidic phospholipids [50]. Besides the occurrence of characteristic phospholipid absorption peaks, further evidence to rule out false positives from the rinsing PBS buffer lies in both the presence of acidic phosphate peaks and the absence of OH vibration peaks in the 3430 $cm^{-1}$ – 3330 $cm^{-1}$ range, which often result from bound water in ionic phosphates such as PBS [50]. Finally, the absence of typical protein peaks in this spectrum again confirms that proteins may not be present on the SIP receptor. **Table 1** shows a summary of the vibration wavenumbers characteristic of proteins and phospholipids as found on the different surfaces. In conclusion, only phospholipids remnants are left on the surface of the SIP during the imprinting process.

To confirm the results of the FTIR experiments, XPS measurements were carried out to check for the presence of the characteristic phosphorus peaks of phosphates [$(PO_4)^{3-}$] at 133.2 eV ($2p_{3/2}$) and 190.7 eV (2s) (**Figure 10**). As shown, these peaks are only present on the two spectra of the SIPs. In particular, the intensity difference between the SIP and the NIP for

both peaks is 25 cpu, approximately. Therefore, the phosphorus present on the SIP must be a result of the imprinting process. In addition, all surfaces were rinsed in PBS followed by a stringent rinsing step with MilliQ water prior to measurements to prevent false positives from the rinsing buffer. The remaining strong peaks around 104.5 eV and 155 eV can be attributed to the excitation of plasmons in the aluminum substrate.

The analysis of the SIP layer for transferred functional groups by both FTIR and XPS has shown that phospholipids, but not proteins, are probably transferred to the SIP layer during imprinting. These results imply that the high contact angle measured on the SIP layer (**Figure 7b**) may be due to remnant lipids, specifically, due to their hydrocarbon chains. Studies show indeed that the presence of such hydrocarbon chains increases surface hydrophobicity. For instance, surfaces modified by either Langmuir-Blodgett monolayers of insoluble double-chain surfactants or single-chain alkanethiols have been demonstrated to be highly hydrophobic, with the degree of hydrophobicity influenced by both the chain ordering and headgroup [35, 51].

It is important to mention that even though yeast cells are structurally different from other cell types, such as mammalian cells, due to the presence of a cell wall on the former, we believe that the conclusions from the FTIR and XPS analyses are also applicable to the latter. For instance, yeast cells, like mammalian cells have a high membrane-protein content in addition to a cell wall-protein content of about 14% by weight [40]. Therefore, the absence of proteins on the SIP is likely not yeast cell-specific. Furthermore, the yeast cell wall does not contain lipids, and consequently, the detected lipids on the SIP indicate that the cell wall maybe trapped in the polymer layer exposing the inner membrane phospholipids on the cavities' surfaces. This appears to not only confirm the assumption that membrane fragments are left in the imprinted cavities (**Figure 4**), but also leads us to conclude that imprinting of mammalian cells and other

eukaryotic cells leaves membrane fragments with exposed phospholipids incorporated onto the SIP surface in a similar manner.

### 3.5 The role of proteins and lipids

To further explore the role played by membrane proteins and phospholipids in the binding of cells to the SIP receptor, HTM monitoring experiments were performed in a manner similar to the initial experiments on SIP and NIP layers described in **Figure 2**. Prior to measuring, yeast SIPs were treated with pepsin to remove any transferred proteins from the SIP. As a control, a NIP was also treated with pepsin in the same manner as the SIP. The pepsin-treated SIP and NIP layers were used in a yeast cell-rebinding study and the result was compared with the result obtained with their non-treated counterparts (**Figure 11a**, and **11b**). As seen in **Figure 11a**, both curves are comparable, suggesting that with regards to the receptor layer, proteins are not involved in binding cells to the surface. Similarly, the pepsin-treated NIP layer showed a similar behavior as a regular NIP (**Figure 11b**).

To study the influence of lipids on the cell-SIP binding mechanisms, a SIP was created using DPPC lipid vesicles as templates and the SIP's ability to bind yeast cells monitored by the HTM. The results obtained are displayed in **Figure 11c**. An $R_{th}$ increase of 1.5 °C/W is produced which is about two times higher than the $R_{th}$ jump measured with a NIP (**Figure 11b)**. This suggests that modifying the surface with lipid moieties promotes cell adhesion. This initial rise in thermal resistance is lower than the increase observed when the cell-imprinted SIP was exposed to a yeast cell suspension, indicating that the non-specific absorption of cells onto a cell-imprinted SIP is higher due to a higher affinity of the template cells towards their imprints. However, upon subsequent rinsing of the SIP imprinted with lipids vesicles, the $R_{th}$ change falls to 42% of the initial increase corresponding to a persistent $R_{th}$ increase of ≈ 0.5 °C/W compared to the baseline, which is similar to the net increase observed on a cell-imprinted SIP. This

suggests that selectivity is driven by the phospholipids moieties that are left behind in the binding cavities.

The ability of lipids to influence cell-substrate adhesion has been reported and is currently being exploited in applications involving medical implants, in which a modification of the implantable material with lipids enhances epithelial cell adhesion [52]. Furthermore, while we demonstrate that lipids on surfaces enhance cell adhesion, Curtis *et al.*, also showed that lipids on the cell membrane equally play a significant role on cell-substrate adhesion [53]. These results, together with the results described in **Figure 7** suggest that the major mechanism by which lipids influence cell-SIP binding might be through hydrophobic forces [54].

## 4. Conclusions

This study has provided further insights into the mechanisms involved in cellular recognition by SIPs. Specifically, selective recognition of cells by SIPs has been shown to depend partly on the geometrical matching between template cells and imprinted cavities on the SIP layer. Such matching ensures a maximal interaction surface between the receptor and the target cell. Furthermore, the interaction between the cells and the cavities appears to be influenced by phospholipids transferred from the cell membrane to the SIP layer. These transferred phospholipids render the cavities hydrophobic, thus, suggesting that lipids play a major role in the SIP recognition mechanism through long-range hydrophobic forces. Conversely, there is no evidence that proteins are transferred to the SIP cavities. Even if proteins were transferred, we show that the recognition of cells by SIP receptors is probably independent of SIP-embedded proteins, since the receptor layer remains effective after treatments of the surface to degrade proteins. However, this does not rule out a role for the surface proteins of the incoming target cell.

While we believe that the results from this study are applicable to the binding of other types of cells to their corresponding SIPs, the study has mostly focused on the chemical and physical modification of the SIP layer due to imprinting and the effect of this modification on the binding of cells from a suspension. Therefore, to provide a complete understanding of the specificity of SIP receptors towards their targets, more research is required. Such research could focus on the influence of cell-surface charge, membrane functional groups on the target cell (carbohydrates, proteins, lipids) and the medium properties on the cell-SIP interaction.

With regards to applications, this study has elucidated some of the major factors that can be controlled to create more efficient SIP layers that are capable of improving the detection limits of SIP-based sensors. In addition, for commercial purposes, it is desirable to develop a synthetic route for the mass production of SIP receptors. In this case, template cells may be replaced by their synthetic analogues. To achieve this, an understanding of the specific molecules that are transferred to the SIP layer and their influence in cell-SIP binding is indispensable. Therefore, the present results bring us a step closer to transferring SIP-based cell detection principles from the proof of concept to commercial applications.

## Acknowledgements

### Biographies

**Derick Yongabi** obtained a Master of Biomedical Science in Bioelectronics and Nanotechnology from the University of Hasselt, Belgium in 2015. Prior to that, he received a Master of Science in Research Methods in 2011 from the University of Leeds, UK. He is currently a PhD student at KULeuven, Belgium, where he works within the Soft Matter and Biophysics section of the department of physics and astronomy. His research exploits interdisciplinary scientific knowledge and tools for understanding biophysical mechanisms with special focus on the development of synthetic receptors and bio(mimetic)sensors.

**Mehran Khorshid** obtained his Doctorate of Veterinary Medicine (DVM) from the Islamic Azad University, Karaj branch, Iran in 2009. Afterwards, he obtained a Master of Biomedical

Sciences in Bioelectronics and Nanotechnology from the University of Hasselt, Belgium in 2014. Currently, he is a PhD student in the Soft-matter and biophysics section of the department of physics and astronomy KULeuven, Belgium. His research interest covers biosensors and biophysical systems.

**Patricia Losada-Pérez** obtained her PhD in Physics from the University of Vigo (Spain) in May 2009. Between 2009 and 2013 she worked as a post-doctoral researcher at the Physics Department of the KULeuven, Belgium. Since 2013 she is a research associate at the Institute of Materials Research of the Hasselt University, Belgium. Her research covers several topics, from thermodynamic equilibrium and non-equilibrium phenomena in condensed and soft matter systems to the fabrication of functional nanostructured materials for biotechnology and energy applications.

**Dr. Kasper Eersels** obtained a master's degree in bioelectronics and nanotechnology from Hasselt University in 2009 and a PhD in science in 2014 at Hasselt University. He worked as a postdoctoral fellow in the BIOSensor group at the same University until 2015. Between 2015 and 2017, he worked as a postdoctoral fellow at KULeuven, Belgium in the Soft Matter and Biophysics section of the department of Physics and Astronomy. Currently, he works at Maastricht University as a postdoc. His research interests cover synthetic receptors and biosensor development, biomedical application engineering and implementation of technologies into a health care settings.

**Olivier Deschaume** obtained his MSc in Physical and Materials Chemistry from the Université de Bourgogne, Dijon, France in 2002. He then moved to the group of Prof. Carole C. Perry at NTU, Nottingham, UK to work in the field of Bio-inspired Materials Chemistry, first as a PhD student and then as a postdoctoral researcher. In 2009, he worked on topics closer to biosensing, surfaces and related characterisation techniques in the groups of Prof. Alain M. Jonas (UCL, 2009-2011) and Carmen Bartic (KUL, 2011 onwards), both located in Belgium. He is now instrument specialist in the Soft Matter Physics and Biophysics unit of KU Leuven, with research interests spanning the fields of biophysics, biosensors, surface science, scanning probe microscopies and bioinspired/bio-assisted materials synthesis.

**Jan D'haen** obtained his PhD in experimental and theoretical study of the behavior of pure iron during the plasma nitriding process. He is a full professor at Hasselt University, Belgium, and for the past 20 years has been responsible for electrical and physical analyses at IMO-IMOMEC

institute, Belgium. His main research interest covers microscopical techniques such as scanning electron microscopy.

**Carmen Bartic** obtained a PhD in Physics from the KU Leuven in collaboration with imec in June 2002 based on her work on organic-based field-effect transducers for bioanalytical applications. Between 2002 and 2009 she was leading the Neuroelectronics research team of imec. In 2007, she was appointed as 10% associate professor at the Department of Physics and Astronomy of the KU Leuven, Belgium. From October 2009, she is full time associate professor in the Soft Matter and Biophysics Unit of the same department at KU Leuven. C. Bartic investigates the properties of bio(nano)materials and their interactions with biomolecules and cells in the context of biosensing applications and has published more than 100 peer-reviewed research articles. She has coordinated several national and international funded projects.

**Jef Hooyberghs** received a master in science, Physics (summa cum laude) in 1998 at KU Leuven, Belgium and obtained a PhD in Physics in 2002 at Hasselt University, Belgium. His doctorate was on non-equilibrium phenomena in statistical physics. Since 2003 he is an employee at VITO (Flemish Institute for Technological Research) and a part time (10%) professor at Hasselt University since 2006. At VITO, he was head the of the research department of Applied Biomolecular Systems from 2012, and recently became the research coordinator of the Health unit. Since 2016 he is member of the Interdisciplinary Expert Panel of the Research Foundation – Flanders (FWO). His research focus is on the thermodynamics of nucleic acid interactions and their applications in bio-detection. He is author of 40+ peer-reviewed papers and 7 patent applications.

**R. Thoelen** obtained his master in applied physics at the TU Eindhoven in 2004. In 2008, he obtained his Ph.D. in Physics at Hasselt university, Belgium on impedance based biosensors. Currently He is an assistant professor at the Faculty of Engineering Technology of Hasselt University since 2013, and is building up a research career within the Institute for Materials Research (IMO-IMOMEC) as a group leader of the research group 'biomedical device engineering'. R. Thoelen is currently the coordinator of the electronics & ICT master program of his faculty and board member of the joint KU Leuven - UHasselt faculty of Engineering Technology. His research interests cover synthesis of materials and their applications in biosensors, as well as the development of various readout techniques for advanced diagnostic applications.

**Michael Wübbenhorst** received his Master and Ph.D. degrees in physics from the University of Leipzig in 1985 and 1989 respectively. In 1990, he joined the Delft University of Technology in The Netherlands as a post-doctoral researcher. In 1995, he became assistant professor in the polymer group at TU Delft. From his position as associate professor (2004) he moved to Belgium where he was appointed at the KU Leuven as professor in experimental soft matter physics in 2005. He also held two temporary positions in Canada (visiting scientist at University of Ontario, Guelph, 2002) and Poland (visiting professor at the Technical University of Lodz, 2008/9). Since 2014 he is head of the Laboratory for Soft Matter and Biophysics (formerly ATF). His scientific interest covers soft matter physics with emphasize on glass forming materials, functional polymers and liquid as well as molecular crystals. He is author of about 165 publications (143 in Web of Science) in high-ranking international journals with more than 3000 citations.

**Patrick Wagner** received his Ph.D. in Physics in 1994 at TU Darmstadt and was postdoctoral researcher at KU Leuven from 1995 till 2001. In 2001, he was appointed as a professor for biophysics at Hasselt University and he returned in 2014 as full professor back to KU Leuven. His main research field is the development of bioanalytical sensors for diagnostic and environmental applications with a special focus on synthetic receptors and thermal detection principles. He has authored or co-authored 250 publications and received several scientific distinctions. Since 2016, P. Wagner is editor-in-chief of the new Elsevier journal Physics-in-Medicine.

This study was financed by the KULeuven project C14/15/066 ‘‘Smart Cellular Scaffolds’’. We gratefully appreciate Drs. Christopher Freiwald of the Institute for Materials Research (IMO) at Hasselt University, for his support on X-ray Photoelectron Spectroscopy. The authors thank Drs. Gideon Wackers, Drs. Peter Cornelis and Drs. Wouter Stilman of the Soft Matter and Biophysics Section, KULeuven, for proofreading and for their insightful comments.

## References

[1] Kramer M, Obermajer N, Matijašić BB, Rogelj I, Kmetec V. Quantification of live and dead probiotic bacteria in lyophilised product by real-time PCR and by flow cytometry. Applied microbiology and biotechnology. 2009 Oct 1; 84(6): 1137-47.

[2] Altamore I, Lanzano L, Gratton E. Dual channel detection of ultra-low concentration of bacteria in real time by scanning fluorescence correlation spectroscopy. Measurement Science and Technology. 2013 May 14; 24(6): 065702.

[3] Hahn MA, Keng PC, Krauss TD. Flow cytometric analysis to detect pathogens in bacterial cell mixtures using semiconductor quantum dots. Analytical chemistry. 2008 Feb 1; 80(3): 864-72.

[4] Krebs MG, Hou JM, Ward TH, Blackhall FH, Dive C. Circulating tumour cells: their utility in cancer management and predicting outcomes. Therapeutic advances in medical oncology. 2010 Nov; 2(6): 351-65.

[5] Schneider B, Vanmeerbeeck G, Stahl R, Lagae L, Bienstman P. Using neural networks for high-speed blood cell classification in a holographic-microscopy flow-cytometry system. InSPIE BiOS 2015 Mar 2 (pp. 93281F-93281F). International Society for Optics and Photonics.

[6] Ramírez-Castillo FY, Loera-Muro A, Jacques M, Garneau P, Avelar-González FJ, Harel J, Guerrero-Barrera AL. Waterborne pathogens: detection methods and challenges. Pathogens. 2015 May 21; 4(2): 307-34.

[7] Eersels K, Lieberzeit P, Wagner P. A Review on Synthetic Receptors for Bioparticle Detection Created by Surface-Imprinting Techniques – From Principles to Applications. ACS Sensors. 2016 Sep 23; 1(10): 1171-87.

[8] Lautner G, Kaev J, Reut J, Öpik A, Rappich J, Syritski V, Gyurcsany RE. Selective Artificial Receptors Based on Micropatterned Surface-Imprinted Polymers for Label-Free Detection of Proteins by SPR Imaging. Advanced Functional Materials. 2011; 21:591-597.

[9] Tretjakov A, Syritski V, Reut J, Boroznjak R, Volobujeva O, Öpik A. Surface molecularly imprinted polydopamine films for recognition of immunoglobulin G. Microchimica Acta. 2013 Nov; 180(15-16): 1433-1442.

[10] Tretjakov A, Syritski V, Reut J, Boroznjak R, Öpik A. Molecularly imprinted polymer film interfaced with Surface Acoustic Wave technology as a sensing platform for label-free protein detection. Analytica Chimica Acta. 2016 Jan 1; 902: 182-188.

[11] Dickert FL, Hayden O, Halikias KP. Synthetic receptors as sensor coatings for molecules and living cells. Analyst. 2001; 126(6): 766-71.

[12] Hayden O, Dickert FL. Selective microorganism detection with cell surface imprinted polymers. Advanced Materials. 2001 Oct 1; 13(19): 1480-3.

[13] Altintas Z, Gittens M, Guerreiro A, Thompson KA, Walker J, Piletsky S, Tothill IE. Detection of waterborne viruses using high affinity molecularly imprinted polymers. Analytical chemistry. 2015 Jun 9; 87(13): 6801-7.

[14] Schirhagl R, Qian J, Dickert FL. Immunosensing with artificial antibodies in organic solvents or complex matrices. Sensors and Actuators B: Chemical. 2012 Oct 31; 173: 585-90.

[15] Tokonami S, Nakadoi Y, Takahashi M, Ikemizu M, Kadoma T, Saimatsu K, Dung LQ, Shiigi H, Nagaoka T. Label-free and selective bacteria detection using a film with transferred bacterial configuration. Analytical chemistry. 2013 Apr 30; 85(10): 4925-9.

[16] van Grinsven B, Eersels K, Akkermans O, Ellermann S, Kordek A, Peeters M, Deschaume O, Bartic C, Diliën H, Steen Redeker E, Wagner P. Label-Free Detection of Escherichia coli Based on Thermal Transport through Surface Imprinted Polymers. ACS Sensors. 2016 Aug 19; 1(9): 1140-7.

[17] Hayden O, Mann KJ, Krassnig S, Dickert FL. Biomimetic ABO Blood- Group Typing. Angewandte Chemie International Edition. 2006 Apr 10; 45(16): 2626-9.

[18] Eersels K, van Grinsven B, Ethirajan A, Timmermans S, Jiménez Monroy KL, Bogie JF, Punniyakoti S, Vandenryt T, Hendriks JJ, Cleij TJ, Daemen MJ. Selective identification of macrophages and cancer cells based on thermal transport through surface-imprinted polymer layers. ACS applied materials & interfaces. 2013 Jul 17; 5(15): 7258-67.

[19] Tai DF, Lin CY, Wu TZ, Huang JH, Shu PY. Artificial receptors in serologic tests for the early diagnosis of dengue virus infection. Clinical chemistry. 2006 Aug 1; 52(8): 1486-91.

[20] Hayden O, Lieberzeit PA, Blaas D, Dickert FL. Artificial antibodies for bioanalyte detection—Sensing viruses and proteins. Advanced Functional Materials. 2006 Jul 4; 16(10): 1269-78.

[21] Ladenhauf EM, Pum D, Wastl DS, Toca-Herrera JL, Phan NV, Lieberzeit PA, Sleytr UB. S-layer based biomolecular imprinting. RSC Advances. 2015; 5(102): 83558-64.

[22] Ramanaviciene A, Ramanavicius A. Molecularly imprinted polypyrrole-based synthetic receptor for direct detection of bovine leukemia virus glycoproteins. Biosensors and Bioelectronics. 2004 Dec 15; 20(6): 1076-82.

[23] Cai D, Ren L, Zhao H, Xu C, Zhang L, Yu Y, Wang H, Lan Y, Roberts MF, Chuang JH, Naughton MJ. A molecular-imprint nanosensor for ultrasensitive detection of proteins. Nature nanotechnology. 2010 Aug 1; 5(8): 597-601.

[24] Wang Y, Zhang Z, Jain V, Yi J, Mueller S, Sokolov J, Liu Z, Levon K, Rigas B, Rafailovich MH. Potentiometric sensors based on surface molecular imprinting:

detection of cancer biomarkers and viruses. Sensors and Actuators B: Chemical. 2010 Apr 8; 146(1): 381-7.

[25] Altintas Z, Pocock J, Thompson KA, Tothill IE. Comparative investigations for adenovirus recognition and quantification: Plastic or natural antibodies?. Biosensors and Bioelectronics. 2015 Dec 15; 74: 996-1004.

[26] Yilmaz E, Majidi D, Ozgur E, Denizli A. Whole cell imprinting based Escherichia coli sensors: A study for SPR and QCM. Sensors and Actuators B: Chemical. 2015 Mar 31; 209: 714-21.

[27] Eersels K, van Grinsven B, Khorshid M, Somers V, Püttmann C, Stein C, Barth S, Diliën H, Bos GM, Germeraad WT, Cleij TJ. Heat-transfer-method-based cell culture quality assay through cell detection by surface imprinted polymers. Langmuir. 2015 Feb 5; 31(6): 2043-50.

[28] Bers K, Eersels K, van Grinsven B, Daemen M, Bogie JF, Hendriks JJ, Bouwmans EE, Püttmann C, Stein C, Barth S, Bos GM. Heat-transfer resistance measurement method (HTM)-based cell detection at trace levels using a progressive enrichment approach with highly selective cell-binding surface imprints. Langmuir. 2014 Mar 19; 30(12): 3631-9.

[29] Stilman W, Jooken S, Wackers G, Cornelis P, Khorshid M, Yongabi D, Akkermans O, Dyson S, van Grinsven B, Cleij T, van Ijzendoorn L, Wagner P, Eersels K. Optimization and Characterization of a Flow Cell for Heat-Transfer-Based Biosensing. *Phys. Status Solidi A*. 2017. DOI: 10.1002/pssa.201600758.

[30] Bossi A, Bonini F, Turner AP, Piletsky SA. Molecularly imprinted polymers for the recognition of proteins: the state of the art. Biosensors and Bioelectronics. 2007 Jan 15; 22(6): 1131-7.

[31] Dickert FL, Hayden O. Bioimprinting of polymers and sol− gel phases. Selective detection of yeasts with imprinted polymers. Analytical chemistry. 2002 Mar 15; 74(6): 1302-6.

[32] Ren K, Banaei N, Zare RN. Sorting inactivated cells using cell-imprinted polymer thin films. ACS nano. 2013 Jul 23; 7(7): 6031.

[33] Losada Pérez P, Jiménez- Monroy KL, van Grinsven B, Leys J, Janssens SD, Peeters M, Glorieux C, Thoen J, Haenen K, De Ceuninck W, Wagner P. Phase transitions in lipid vesicles detected by a complementary set of methods: heat- transfer measurements, adiabatic scanning calorimetry, and dissipation- mode quartz crystal microbalance. physica status solidi (a). 2014 Jun 1; 211(6): 1377-88.

[34] Nakano T, Kikugawa G, Ohara T. A molecular dynamics study on heat conduction characteristics in DPPC lipid bilayer. The Journal of chemical physics. 2010 Oct 21; 133(15): 154705.

[35] Kalay N. Interfacial Dynamics. New York: Marcel Dekker Inc; 2000.

[36] Alsteens D, Dague E, Rouxhet PG, Baulard AR, Dufrêne YF. Direct measurement of hydrophobic forces on cell surfaces using AFM. Langmuir. 2007 Nov 20; 23(24): 11977-9.

[37] Van Loosdrecht MC, Lyklema J, Norde W, Schraa G, Zehnder AJ. The role of bacterial cell wall hydrophobicity in adhesion. Applied and environmental microbiology. 1987 Aug 1; 53(8): 1893-7.

[38] Klotz SA, Drutz DJ, Zajic JE. Factors governing adherence of Candida species to plastic surfaces. Infection and immunity. 1985 Oct 1; 50(1): 97-101.

[39] Henriques M, Gasparetto K, Azeredo J, Oliveira R. Experimental methodology to quantify Candida albicans cell surface hydrophobicity. Biotechnology letters. 2002 Jul 1; 24(13): 1111-5.

[40] Nguyen TH, Fleet GH, Rogers PL. Composition of the cell walls of several yeast species. Applied microbiology and biotechnology. 1998 Aug 16; 50(2): 206-12.

[41] Pergal MV, Džunuzović JV, Poręba R, Micić D, Stefanov P, Pezo L, Špírková M. Surface and thermomechanical characterization of polyurethane networks based on poly (dimethylsiloxane) and hyperbranched polyester. Express Polymer Letters. 2013 Oct 1; 7(10).

[42] Zhang C, Ren Z, Yin Z, Qian H, Ma D. Amide II and amide III bands in polyurethane model soft and hard segments. Polymer Bulletin. 2008 Feb 9; 60(1): 97-101.

[43] Abramson MB, Norton WT, Katzman R. Study of ionic structures in phospholipids by infrared spectra. Journal of Biological Chemistry. 1965 Jun 1; 240(6): 2389-95.

[44] Socrates G. Infrared and Raman characteristic group frequencies: table and charts. Ltd WJS. 2001: 1-347.

[45] Van der Rest ME, Kamminga AH, Nakano A, Anraku Y, Poolman B, Konings WN. The plasma membrane of Saccharomyces cerevisiae: structure, function, and biogenesis. Microbiological reviews. 1995 Jun 1; 59(2): 304-22.

[46] Ami D, Posteri R, Mereghetti P, Porro D, Doglia SM, Branduardi P. Fourier transform infrared spectroscopy as a method to study lipid accumulation in oleaginous yeasts. Biotechnology for biofuels. 2014 Jan 23; 7(1): 12.

[47] Meng X, Pan Q, Ding Y, Jiang L. Rapid determination of phospholipid content of vegetable oils by FTIR spectroscopy combined with partial least-square regression. Food chemistry. 2014 Mar 15; 147: 272-8.

[48] Wang HP, Wang HC, Huang YJ. Microscopic FTIR studies of lung cancer cells in pleural fluid. Science of the Total Environment. 1997 Oct 1; 204(3): 283-7.

[49] Matthäus C, Bird B, Miljković M, Chernenko T, Romeo M, Diem M. Infrared and Raman microscopy in cell biology. Methods in cell biology. 2008 Dec 31; 89: 275-308.

[50] Gremlich U, Yan B. Infrared and Raman spectroscopy of biological materials. New York: Marcel Dekker Inc; 2001.

[51] Rabinovich YI, Guzonas DA, Yoon RH. Role of chain order in the long-range attractive force between hydrophobic surfaces. Langmuir. 1993 May; 9(5): 1168-70.

[52] Levy RJ, Alferiev I, Stachelek SJ, inventors; The Children's Hospital of Philadelphia, assignee. Steroid lipid-modified polyurethane as an implantable biomaterial, the preparation and uses thereof. United States patent US 8,465,542. 2013 Jun 18.

[53] Curtis AS, Chandler C, Picton N. Cell surface lipids and adhesion. III. The effects on cell adhesion of changes in plasmalemmal lipids. Journal of cell science. 1975 Aug 1; 18(3): 375-84.

[54] Helm CA, Israelachvili JN, McGuiggan PM. Molecular mechanisms and forces involved in the adhesion and fusion of amphiphilic bilayers. science. 1989 Nov 17; 246(4932): 919-23.

Figure Caption

**Captions**

**Figure 1** The HTM set up used to detect cells. Bound cells block thermal transport through the SIP-liquid interface. This results in an increase in the heat transfer resistance, $R_{th}$, which causes a decrease in the liquid temperature, $T_2$. $T_2$ and $T_1$ are measured by thermocouples and together with the supplied power, are used to determine the time-dependent $R_{th}$ response at the receptor-liquid interface.

**Figure 2** Binding $R_{th}$ response by the HTM method. **(a)** A small, reversible increase in thermal resistance is measured on the NIP layer **(b)**. The $R_{th}$ response acquired with a yeast SIP showing a higher $R_{th}$ increase, which is not fully reversed after flushing.

**Figure 3 (a)** AFM image of a non-extracted SIP showing stamped template yeast cells. **(b)** Corresponding SEM image of a non-extracted yeast-imprinted polymer layer. **(c)** AFM image of a yeast SIP receptor produced after cell extraction showing cavities geometrically comparable to the cells. **(d)** SEM image of a yeast SIP upon cell extraction confirms the geometrical match between cells and the imprinted cavities shown in the AFM image.

**Figure 4** SEM image of a yeast-imprinted cavity revealing nano-scale roughness within the cavity.

**Figure 5** AFM image of silica-imprinted cavities on a polyurethane surface, showing cavities geometrically identical to the 2 μm-silica templates.

**Figure 6** Images of polymer layers after exposure to a 10 mg/ml suspension of yeast cells followed by a 12 minutes rinsing step in the HTM device. **(a)** AFM image of a yeast SIP layer revealing bound yeast cells. **(b)** SEM image of a yeast SIP equally showing bound yeast cells

in cavities and confirming AFM results. **(c)** SEM image of a NIP surface without cells after a similar experiment.

**Figure 7** Wetting behaviour of different polymer surfaces measured by water contact angle. **(a)** Contact angle of a non-extracted yeast SIP layer. **(b)** Contact angle of a yeast SIP. **(c)** Contact angle of a NIP. **(d)** Contact angle of polyurethane layer imprinted with silica beads.

**Figure 8** FTIR spectra of non-extracted yeast SIP, yeast SIP and NIP. The insert shows the C=O stretching vibration bands in more details for each of the layers under study.

**Figure 9** **(a)** Difference between a SIP and NIP spectrum showing peaks typical of phospholipids. **(b)** Enlarged view of the phosphate region of the SIP-NIP spectrum showing the different vibrational wavenumbers of the phosphate head group.

**Figure 10** XPS spectra obtained for a non-extracted yeast SIP, yeast SIP and NIP. The results indicate that phosphorus is present on the SIP but not on the NIP.

**Figure 11** HTM investigation of the role of proteins and phospholipids in the cell-SIP binding mechanism. **(a)** $R_{th}$ response of a yeast SIP and a pepsin-treated yeast SIP layer at 37 °C. The pepsin treatment does not degrade the SIP's ability to bind template cells. (b) $R_{th}$ response of a NIP and a pepsin-treated NIP layer at 37 °C showing a similar $R_{th}$ behavior for both. **(c)** $R_{th}$ response of a SIP layer created using 400 nm DPPC phospholipid vesicles as the template.

**Figures**

**Fig. 1**

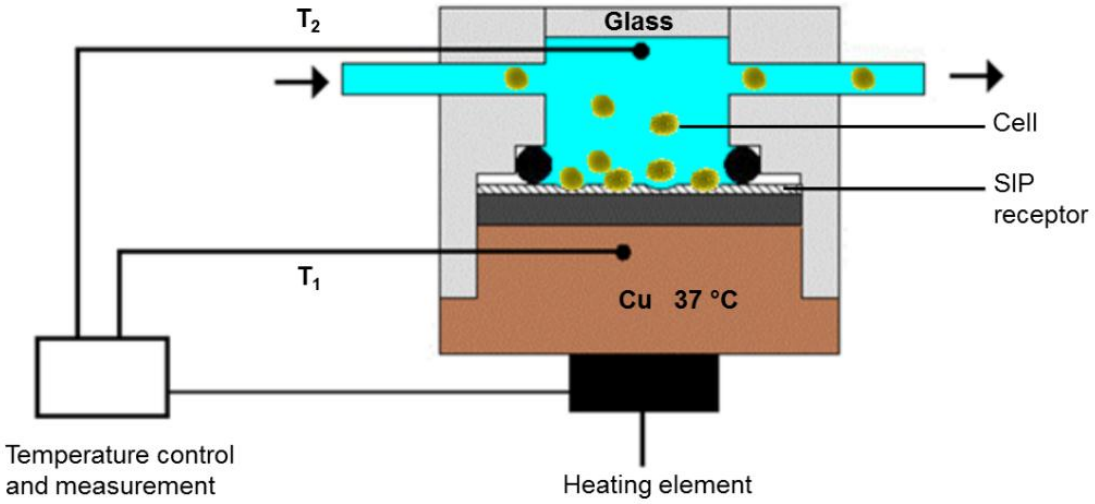


**Fig. 2**

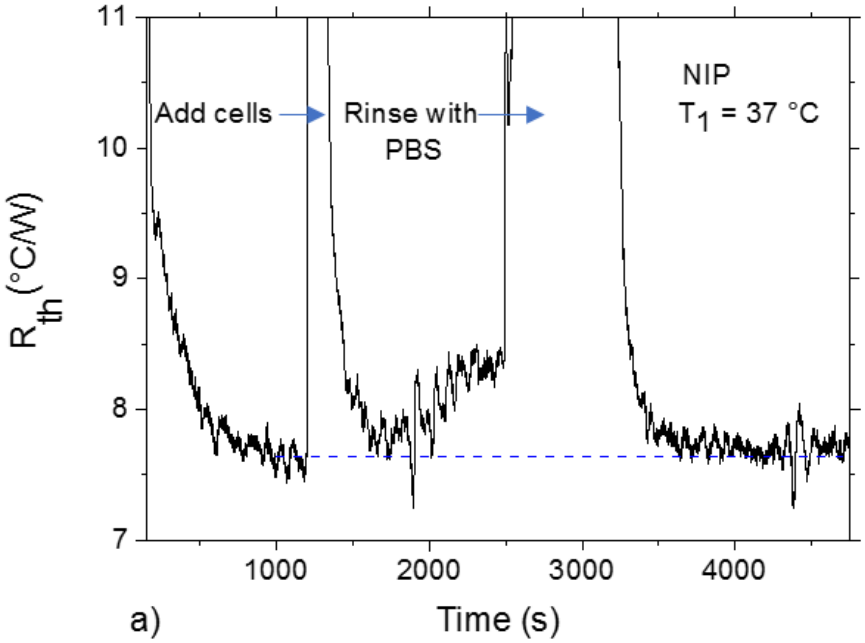

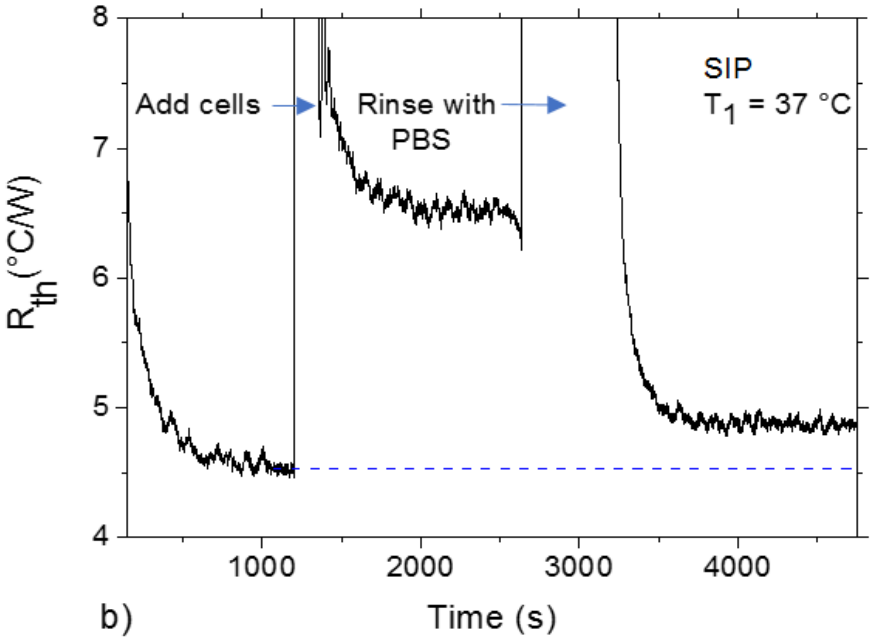


**Fig. 3**

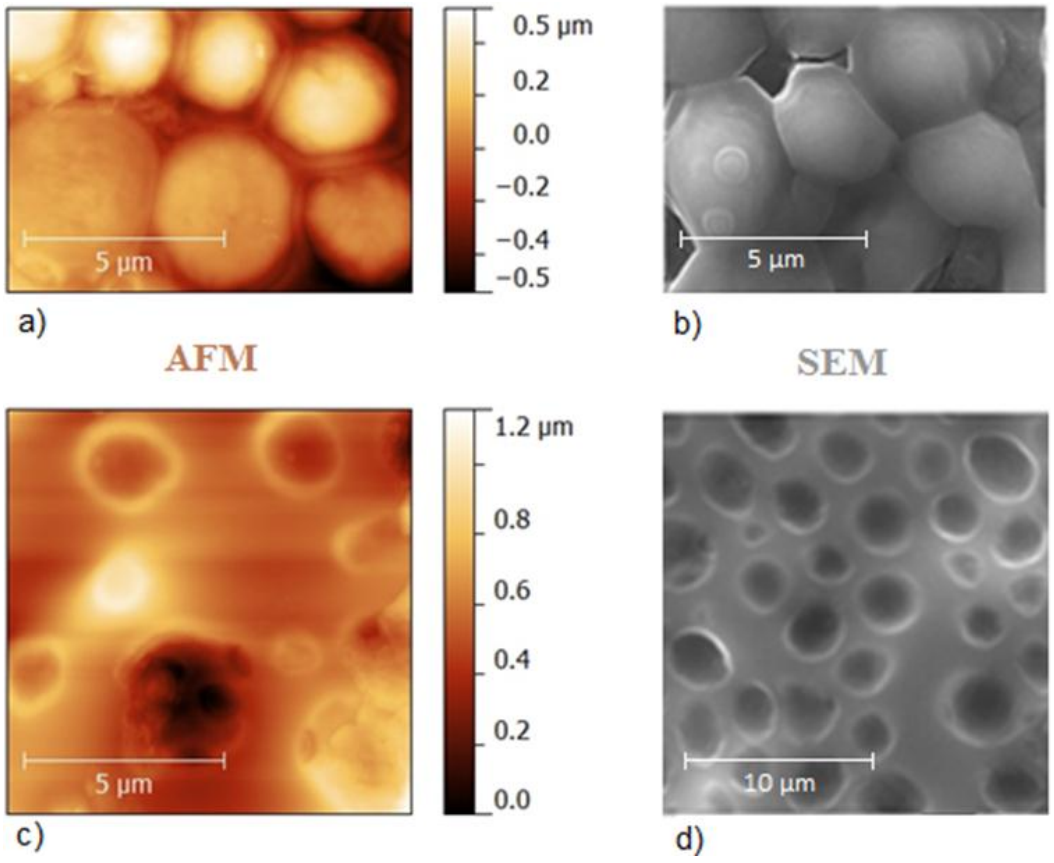


**Fig. 4**

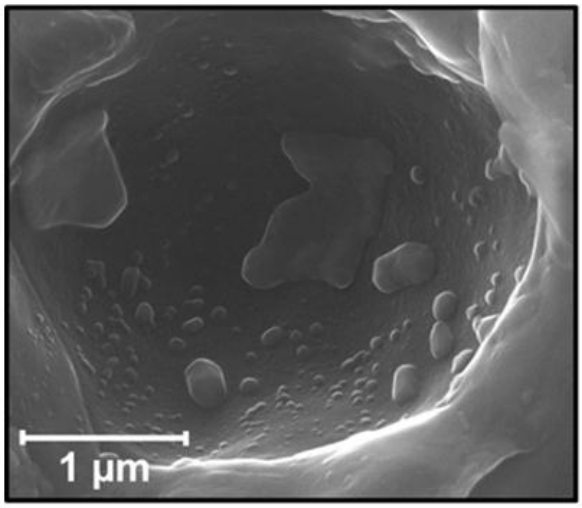


**Figure 5**

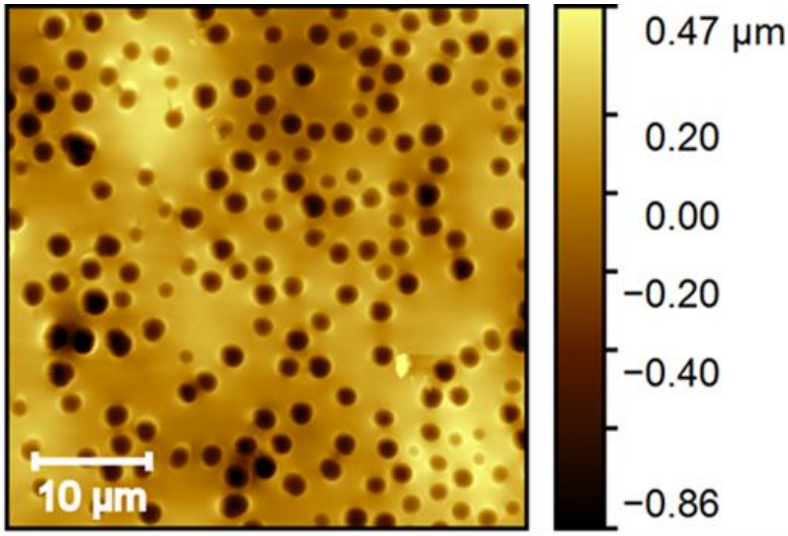


**Fig. 6**

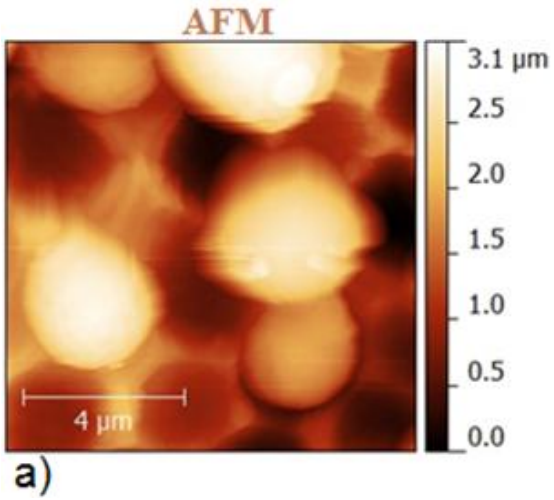

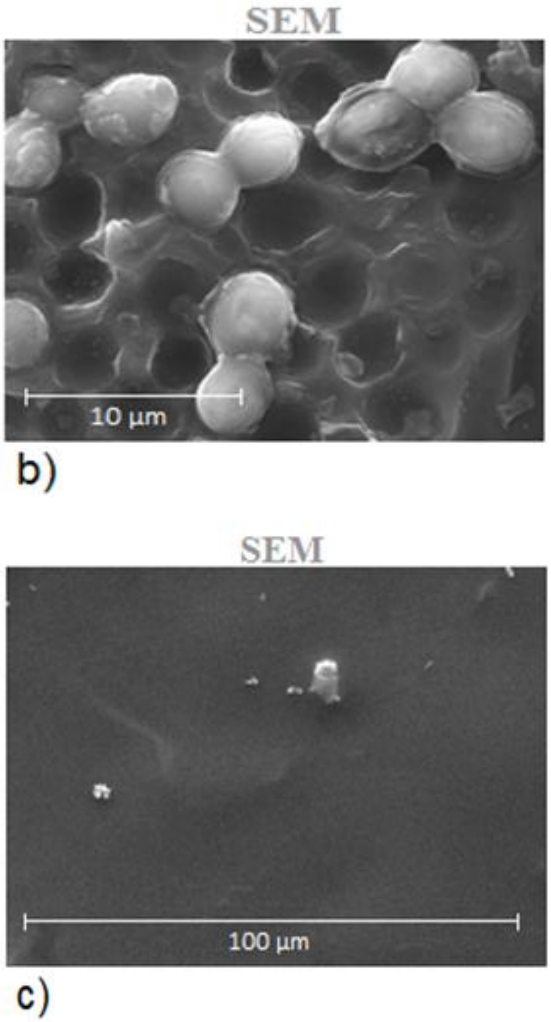


**Fig. 7**

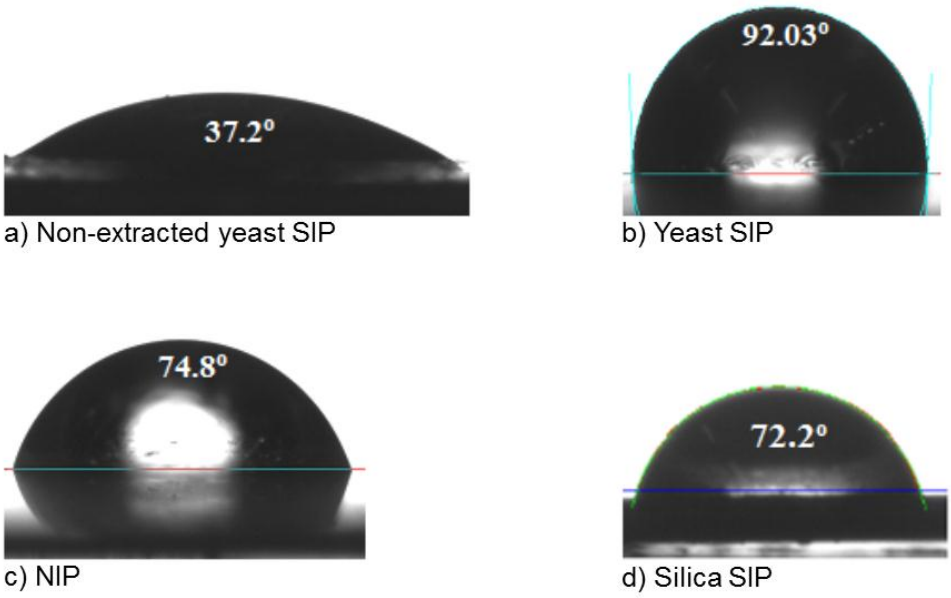


**Fig. 8**

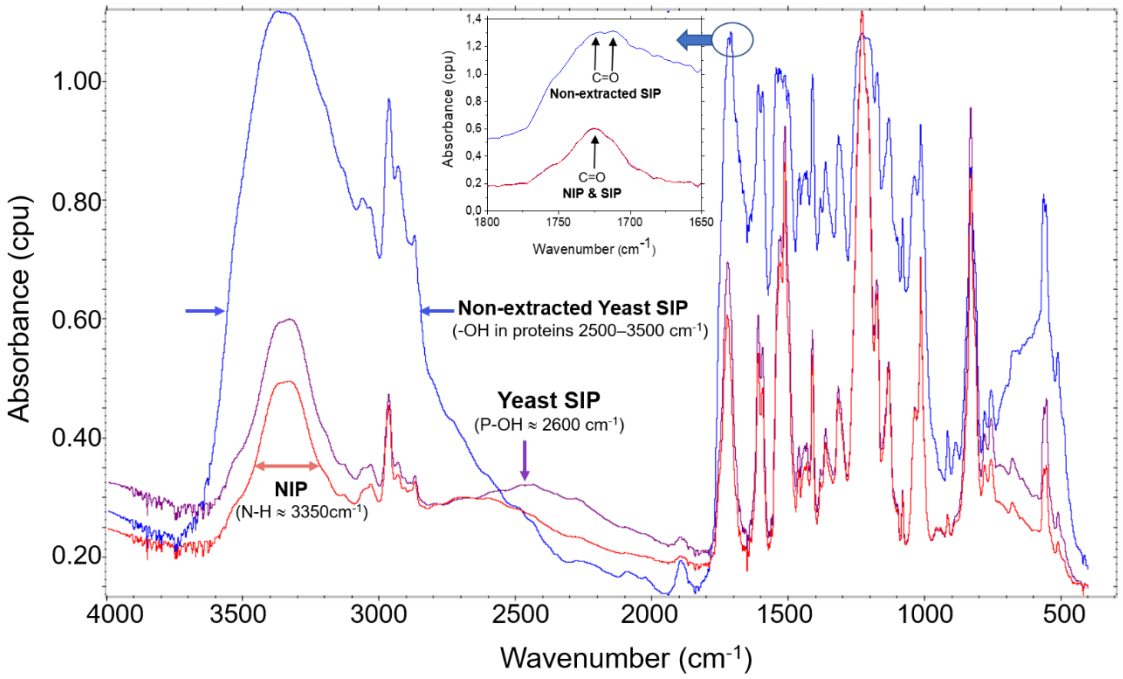


**Fig. 9**

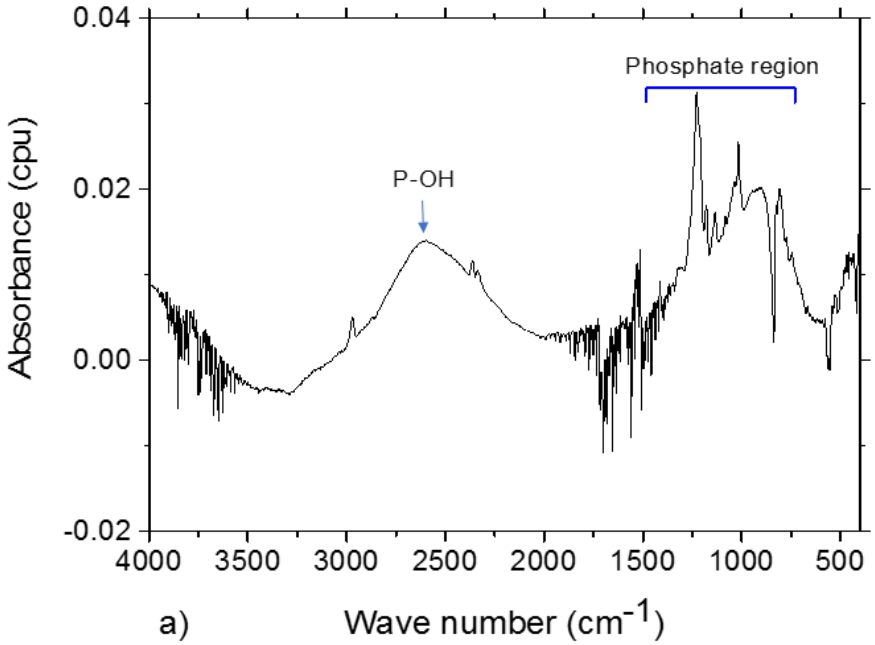

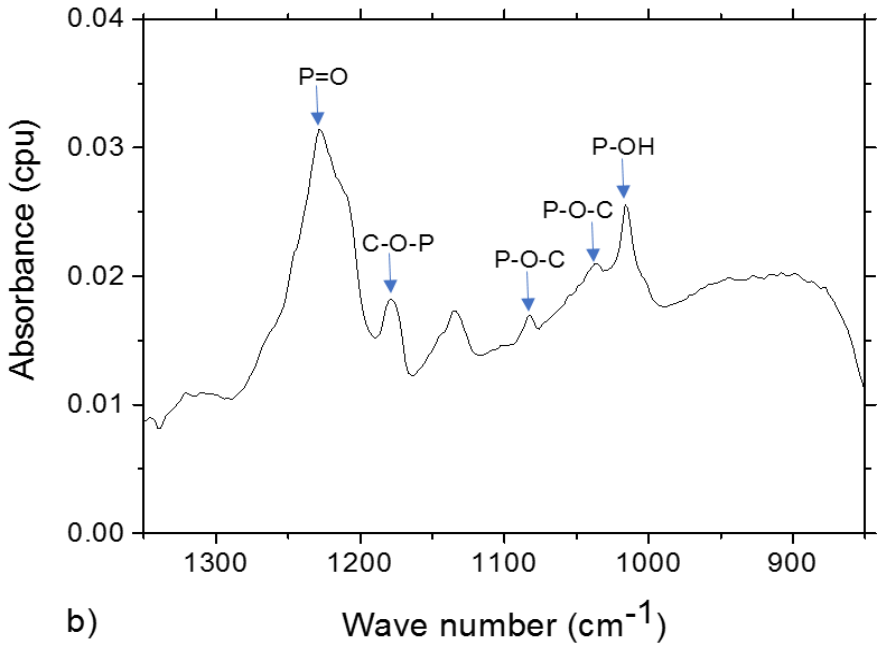


**Fig. 10**

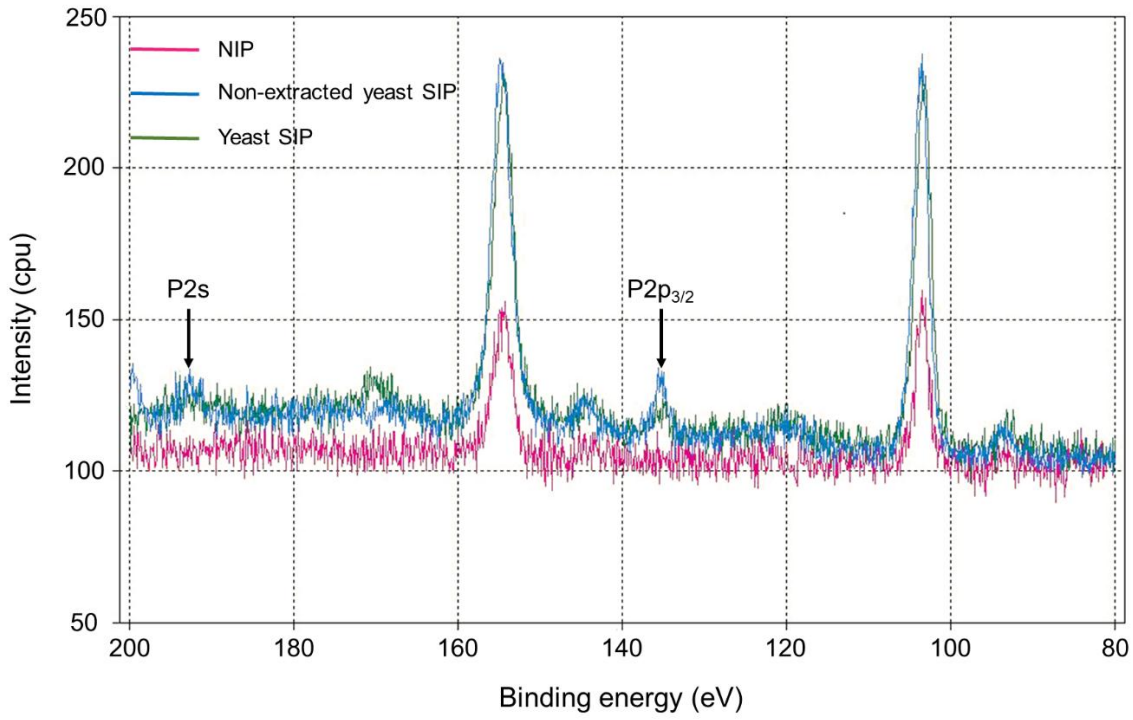


**Fig. 11**

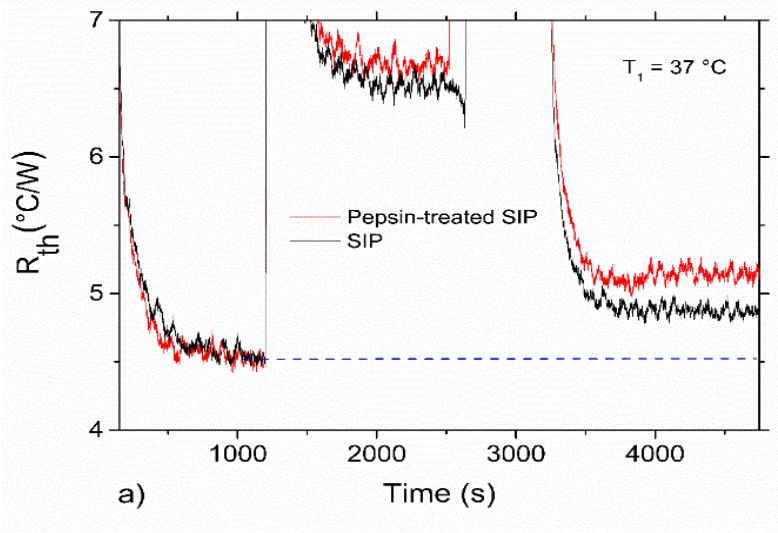


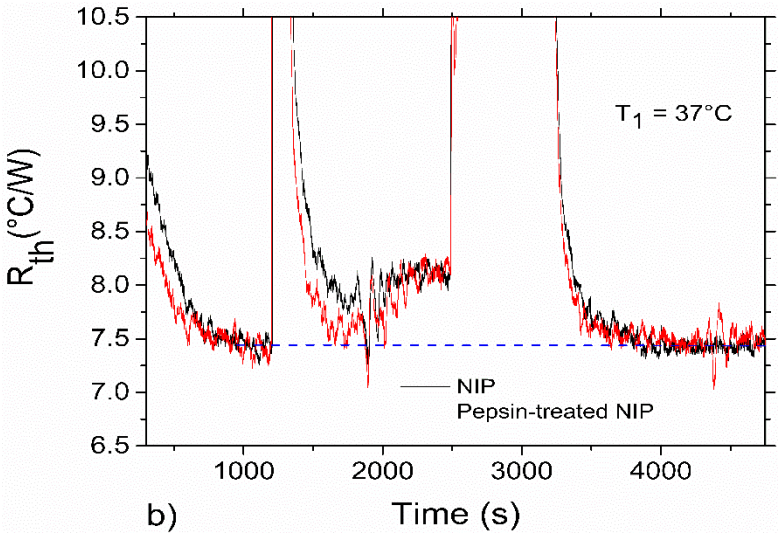


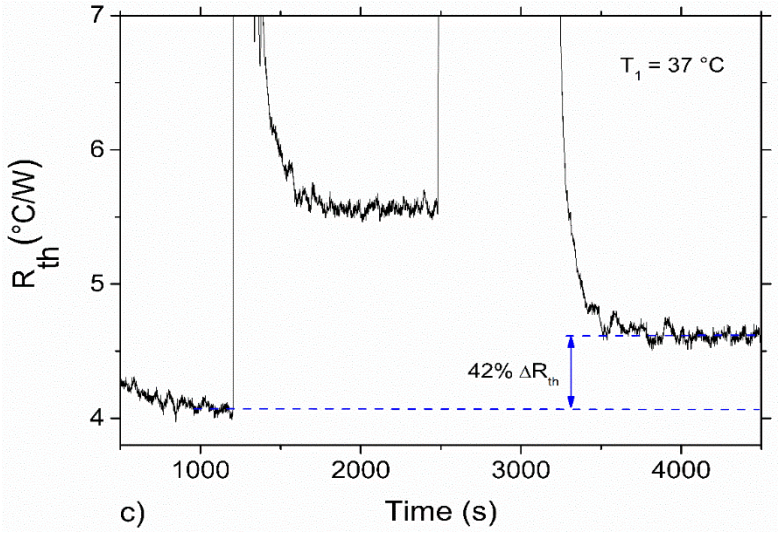

| Functional class | Vibration bands | Wave number ($cm^{-1}$) | Non-extracted yeast SIP | Yeast SIP | NIP |
|---|---|---|---|---|---|
| **Carboxylic acids (proteins)** | **O-H** | 2500-3350 * | √ | × | × |
| | **C=O** (Double bands) | 1710 – 1729 | √ | × | × |
| **Phospholipids** | **P-OH** | 2600, 1014 | √ | √ | × |
| | **$PO_2^-$** (Asymmetric) | 1232 | √ | √ | × |
| | **$PO_2^-$** (Symmetric) | 1080 | √ | √ | × |
| | **C-O-P** in C-O-$PO_2^-$ (Symmetric) | 1180 | √ | √ | × |
| | **P-O-C** (Symmetric) | 1035 | √ | √ | × |

**Table 1** Vibration wavenumbers characteristic of proteins and phospholipids as found on the different surfaces, non-extracted yeast SIP, yeast SIP and NIP.

√ Yes × No
* Very broad peak with overlapping C-H bands is typical for carboxylic acids